STRUCTURAL CHARACTERIZATION OF ELECTROSPUN SCAFFOLDS BY IMAGE ANALYSIS TECHNIQUES

Elham Vatankhah, Dariush Semnani
Mahdi Tadayon

Department of Textile Engineering, Isfahan University of Technology, Isfahan, 84156-83111, Iran
Behrad Consulting Engineers Co., Isfahan, Iran

ABSTRACT

Understanding the influence of electrospun scaffold architecture (fiber diameter, pore size, and fiber orientation) on morphology, adhesion, proliferation, differentiation and organization of different kinds of cells and mechanical behavior leads to engineering the functional tissue for reconstruction by controlling the electrospinning process. Quantifying the fiber architectural features provides the ability to access this influence.
The aim of this research is characterizing the electrospun scaffold topology including fiber diameter, pore size and fiber orientation using an image-based analysis approach. To investigate the algorithm performance, the images of electrospun polycaprolactone scaffolds using scanning electron microscopy (SEM) were prepared.
This image-based analysis technique not only combines fast and precise analysis of computer-based programs but also makes the reliable results to identify the fiber network morphology.

Index Terms—image processing, topology, electrospun scaffolds

1. INTRODUCTION

Electrospun fibrous scaffolds are widely used in tissue engineering due to their similarity to extracellular matrix (ECM) fibrils in both dimension and morphology [1,2]. Depending on the materials used and electrospinning conditions, nonwoven fibrous meshes with microscale variation, for instance, in pore size and fiber diameter have been successfully produced [2]. In addition, this technology offers the ability to control scaffold composition, structure, and mechanical properties [3,4,5]. Biological properties of scaffolds can be tailored to specific applications by controlling fiber identity and alignment [6]. Multiple types of electrospun fibers such as random [7,8], aligned [9,10,11,12,13], and porous structures [14] are capable of supporting the attachment and proliferation of a variety of cell types and guiding their bahavior[15]. For example, it is found that human coronary artery smooth muscle cells (SMCs) attached and migrated along the axis of the aligned nano fibers and expressed a spindle-like contractile phenotype [16]. The effect of fiber diameter on cell proliferation has also been explored, with the general conclusion that smaller fibers seem to encourage better cell replication and signalling [17,18,19]. The effect of pore size and porosity on cell growth is of particular relevance, as the utilization of space is a key concern in the use of electrospun mats as tissue engineering templates [19].
Understanding the influence of electrospun scaffold architecture (fiber diameter, fiber orientation distribution and pore size) on morphology, adhesion, proliferation, differentiation and organization of different kinds of cells and mechanical behavior leads to engineering the functional tissue for regeneration by controlling the electrospinning process. Quantifying the fiber architectural features provides the ability to access this influence.
The aim of this research is characterizing the electrospun scaffold topology including fiber diameter, fiber orientation distribution and pore size using an image-based analysis approach. To investigate the algorithm performance the images of electrospun polycaprolactone scaffolds using scanning electron microscopy (SEM) were prepared.

2. APPROACH

2.1. Materials and Scaffold Fabrication

Polycaprolactone (PCL) (M_w= 70,000- 90,000) was purchased from Sigma- Aldrich and dimethylformamide (DMF) and methylene chloride were obtained from Merck.
The polymer solution with concentration of 11% w/v was prepared by dissolving PCL in a 4:1 mixture of methylene chloride and DMF under stirring for 24h at room temperature. The solution was electrospun from a 5 ml syringe with a needle diameter of 0.6 mm and flow rate of 2 ml/h. A positive voltage (16 kV) was applied to the polymer solution and the distance between the syringe tip and the collecting mandrel was 12 cm and the rotation rate was approximately 500 rpm.

2.2. Image Analysis Algorithm

2.2.1. Image Preprocessing

For imaging, each PCL specimen was sputter- coated with gold and imaged (grayscale) using a standard scanning electron microscopy (SEM) (XL30, Philips, Netherlands). The specimens were imaged at 6000 x magnification.

The method uses a grayscale image as an input. Then, median and Wiener filters are used for preprocessing the image. The median filter is a nonlinear digital filtering technique that preserves edges while removing noise [20]. Wiener filtering is one of the earliest and best known approaches to linear image restoration [21]. The purpose of Wiener filter is to reduce the amount of noise present in a signal by comparison with an estimation of the desired noiseless signal [22].

Sobel operator is used in the next step to calculate the gradient's direction for each point (x, y). In simple terms, the operator calculates the gradient of the image intensity at each point, giving the direction of the largest possible increase from light to dark and the rate of change in that direction. Mathematically, the operator uses two 3×3 kernels which are convolved with the original image to calculate approximations of the derivatives- one for horizontal changes and one for vertical. If we define A as the source image, and G_x and G_y are two images which at each point contain the horizontal and vertical derivative approximations, the computations are as follows:

$$G_y = \begin{bmatrix} -1 & -2 & -1 \\ 0 & 0 & 0 \\ +1 & +2 & +1 \end{bmatrix} * A \quad (1)$$

$$G_x = \begin{bmatrix} -1 & 0 & +1 \\ -2 & 0 & +2 \\ -1 & 0 & +1 \end{bmatrix} * A \quad (2)$$

where * here denotes the 2- dimensional convolution operation. The x- coordinate is here defined as increasing in the "right"- direction, and the y- coordinate is defined as increasing in the "down"- direction. At each point in the image, the resulting gradient approximations can be combined to give the gradient magnitude, using:

$$G = \sqrt{G_x^2 + G_y^2} \quad (3)$$

Using this information, we can also calculate the gradient's direction [23]:

$$\theta = \arctan\left(\frac{G_y}{G_x}\right) \quad (4)$$

2.2.2. Fiber Diameter Detection

To simplify, the obtained gradient's directions of image according to Table 1 are replaced by 0, 45, 90 and 135 degrees.

Table 1. Simplifying the obtained gradient's directions

Real Value	Replacement Value
0≤θ<22.5	θ=0
22.5≤θ<67.5	θ=45
67.5≤θ<112.5	θ=90
112.5≤θ<157.5	θ=135
157.5≤θ<180	θ=0

The next step is detecting the edge of fibers in the image using Canny method. So, the binary image which has white pixels in fiber edges is created by Canny.

The Canny detector is the most powerful edge detector provided by function edge [21].

To find the fiber diameter, the algorithm starts from a white pixel and scans the binary image pixel by pixel to find the next white pixel. The number of counted pixels represents the fiber diameter. If θ equals 0° and 90° scanning direction will be towards X and Y axes, respectively. If θ equals 45° or 135° moving direction will be towards the corresponding angle (Figure1). To minimize the calculation error, there are scanning limitations in number of counting pixels and direction of two white pixels.

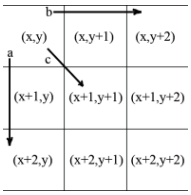


Figure 1. Scanning direction to calculate fiber diameter (a)for θ=0°, (b) for for θ=90° and (c) for for θ=45°, 135°.

2.2.3. Fiber Orientation

After calculating the gradient's direction of each pixel using Sobel operator, Canny detector is used to detect the edge of fibers and make a binary image. The direction of fiber edge pixels being white are classified into 36 categories.

2.2.4. Pore Size

After applying Wiener filter, the image is inversed. Then the image is converted into a binary image by using a threshold obtained by trial and error method. The function regionprops in MATLAB is used to extract features of the voids including region number, region bounding box, region centroid and region area.

Function regionprops is IPT's principal tool for computing region descriptors [21].

3. RESULTS AND DISCUSSION

Figures 2 and 3 show the input and binary images, respectively.

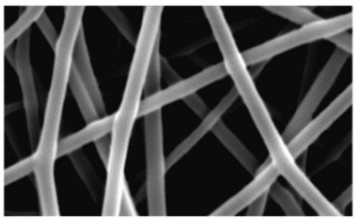


Figure 2. Input image



Figure 3. Binary image obtained by Canny detector

3.1. Fiber Diameter Detection

Fiber diameter distributions for the image given in Figure 2 obtained by described methods is shown in Figure 4. Calculated mean and standard deviation of fiber diameter are 32.36 and 5.8 pixels, respectively.

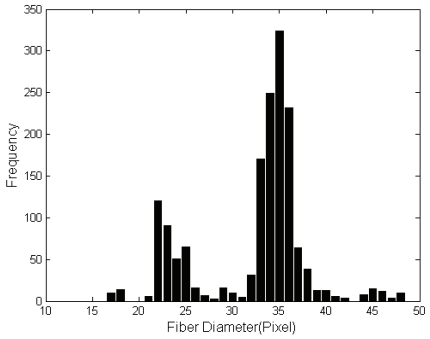


Figure 4. Fiber diameter distribution

3.2. Fiber Orientation

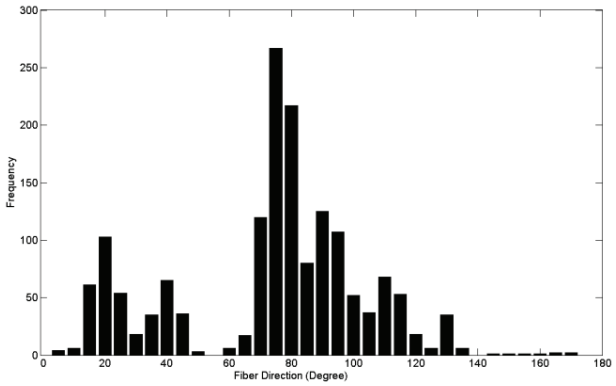


Figure 5. Fiber orientation distribution

Fiber orientation is shown in Figure 5. Figure 6 exhibits the fiber orientation vs fiber diameter. This diagram indicates that in mentioned fabrication condition (in scaffold fabrication section), the frequency of fibers with diameter and direction between 32.5 to 35.5 pixels and 70 to 88 degrees, respectively is more than other states.

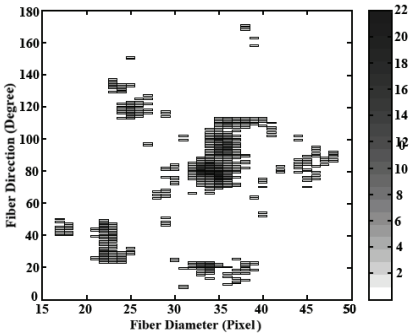


Figure 6. Fiber direction vs fiber diameter

3.3. Pore Size

Figure 8 depicts the pore sizes detected in *Figure 7*. Mean and standard deviation of pore size obtained using mentioned method are 9.42×10^4 and 7.27×10^4 pixels, respectively.

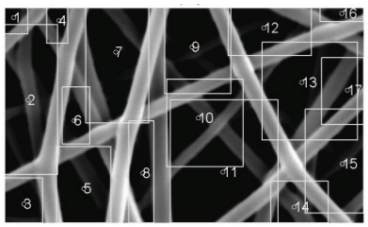


Figure 7. Pores detection (pore number, pore bounding box and pore centroid)

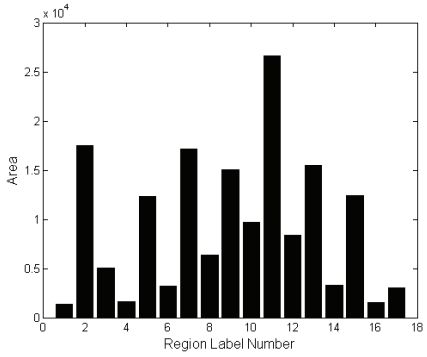


Figure 8. Pore area

4. CONCLUSION

In this study, a new image analysis based method for assessing electrospun topology was successfully developed. This automatic procedure in comparison with manual method guarantees significant accuracy and reduction in

analysis time as well as it has the capability of being used as an on-line technique for quality control.

5. REFERENCES

[1] B. Subia, J. Kundu, and S.C. Kundu, "Biomaterial scaffold fabrication techniques for potential tissue engineering applications", *Tissue Engineering*, Eberli D. (ed.), In- Teh, pp. 141-157, 2010.

[2] X. Yang, and H. Wang, "Electrospun Functional Nanofibrous Scaffolds for Tissue Engineering", *Tissue Engineering*, Eberli D. (ed.), In- Teh, pp. 159-177, 2010.

[3] J.S. Choi , S.J. Lee, G.J.Christ, A. Atala, and J.J. Yoo, "The influence of electrospun aligned poly(ε-caprolactone)/collagen nanofiber meshes on the formation of self-aligned skeletal muscle myotubes", *Biomaterials*, Vol. 29, No. 19, pp. 2899-2906, 2008.

[4] J.Stitzel, J. Liu, S.J. Lee, M. Komura, J. Berry, S. Soker , G. Lim, M. Van Dyke, R. Czerw, J.J. Yoo, and A. Atala, "Controlled fabrication of a biological vascular substitute", *Biomaterials*, Vol. 27, No. 7, pp. 1088-1094, 2006.

[5] S.J. Lee, J J. Yoo, G. Lim, A. Atala, and J. Stitzel, "In vitro evaluation of electrospun nanofiber scaffolds for vascular graft application", *Journal of Biomedical Materials Research Part A*, Vol. 83, No. 4, pp. 999-1008, 2007.

[6] C.E. Ayres, G.L. Bowlin, R. Pizinger, L.T. Taylor, C.A. Keen, and D.G. Simpson, "Incremental changes in anisotropy induce incremental changes in the material properties of electrospun scaffolds", *Acta Biomaterialia*, Vol. 3, No. 5, pp. 651-661, 2007.

[7] C.M. Vaz, S. van Tuijl, C.V.C. Bouten, and F.P.T. Baaijens, "Design of scaffolds for blood vessel tissue engineering using a multi-layering electrospinning technique" *Acta Biomaterialia*, Vol. 1, No. 5, pp. 575-582, 2005.

[8] K.S. Rho, L. Jeong, G. Lee, B.M. Seo, Y.J. Park, S.D. Hong, S. Roh, J.J. Cho, W.H. Park, and B. Min, "Electrospinning of collagen nanofibers: Effects on the behavior of normal human keratinocytes and early-stage wound healing", *Biomaterials*, Vol. 27, No. 8, pp. 1452-1461, 2006.

[9] J. M. Corey, D.Y. Lin, K.B. Mycek, Q. Chen, S. Samuel, E.L. Feldman, and D.C. Martin, "Aligned electrospun nanofibers specify the direction of dorsal root ganglia neurite growth", *Journal of Biomedical Materials Research Part A*, Vol. 83, No. 3, pp. 636-645, 2007.

[10] J.M. Corey, C.C. Gertz, B. Wang, L.K. Birrell, S.L. Johnson, D.C. Martin, and E.L. Feldman, "The design of electrospun PLLA nanofiber scaffolds compatible with serum-free growth of primary motor and sensory neurons", *Acta Biomaterialia*, Vol. 4, No.4, pp. 863-875, 2008.

[11] H.B. Wang, M.E. Mullins, J.M. Cregg, A. Hurtado, M. Oudega, M.T. Trombley, and R.J. Gilbert, "Creation of highly aligned electrospun poly-L-lactic acid fibers for nerve regeneration applications", *Journal of Neural Engineering*, Vol. 6, No. 1: 016001, 2009.

[12] J. Xie, M.R. MacEwan, X. Li, S.E. Sakiyama-Elbert, and Y. Xia, "Neurite Outgrowth on Nanofiber Scaffolds with Different Orders, Structures, and Surface Properties", *ACS Nano*, Vol. 3,No. 5, pp. 1151-1159, 2009.

[13] F. Yang, R. Murugan, S. Wang, and S. Ramakrishna, "Electrospinning of nano/micro scale poly(L-lactic acid) aligned fibers and their potential in neural tissue engineering", *Biomaterials*, Vol. 26, No. 15, pp. 2603-2610, 2005.

[14] J.T. McCann, D. Li, and Y. Xia, "Electrospinning of nanofibers with core-sheath, hollow, or porous structures", *Journal of Materials Chemistry*, Vol. 15, No. 7, pp. 735-738, 2005.

[15] H. B. Wang, M. E. Mullins, J. M. Cregg, C. W. McCarthy, and R. J. Gilbert, "Varying the diameter of aligned electrospun fibers alters neurite outgrowth and Schwann cell migration", *Acta Biomaterialia*, Vol. 6, No. 8, pp. 2970-2978, 2010.

[16] D. Lian, B.S. Hsiao, and B. Chu, "Functional electrospun nanofibrous scaffolds for biomedical applications", *Advanced Drug Delivery Reviews*, Vol. 59, No. 14, pp. 1392–1412, 2007.

[17] I.K. Kwon, S. Kidoaki, and T. Matsuda, "Electrospun nano- to microfiber fabrics made of biodegradable copolyesters: structural characteristics, mechanical properties and cell adhesion potential, *Biomaterials*, Vol. 26, No. 18, pp. 3929-3939, 2005.

[18] G.T. Christopherson, H. Song, and H.Q. Mao, "The influence of fiber diameter of electrospun substrates on neural stem cell differentiation and proliferation", *Biomaterials*, Vol. 30, No. 4, pp. 556-564, 2009.

[19] J. L. Lowery, N. Datta, and G.C. Rutledge, "Effect of fiber diameter, pore size and seeding method on growth of human dermal fibroblasts in electrospun poly(ε-caprolactone) fibrous mats", *Biomaterials*, Vol. 31, No. 3, pp. 491–504, 2010.

[20] S.K. Satpathy, S. Panda, K.K. Nagwanshi, S.K. Nayak, and S. Ardil, "Adaptive Non-linear Filtering Technique for Image Resoration", *International Journal of Electrical and Computer Engineering*, Vol. 5, No. 1, pp. 15- 22, 2010.

[21] R. C. Gonzalez, R. E. Woods, S. L. Eddins, *Digital Image Processing Using MATLAB*, Gatesmark Publishing, Knoxville, TN, USA, 2009.

[22] C. Chen, L. Si, Z. Yang, "SNR Estimation for Wiener Filter in OFDM System", *3rd International Congress on Image and Signal Processing (CISP2010)*, pp. 4441- 4444, 2010.

[23] A.M. Bhugul, V.K. Shandilya, "Preserving Image Features by Removing Noise through Diffusion Filtering", *International Journal of Engineering and Technoscience*, Vol. 2, No. 1, pp. 114-119, 2011.